01

Quasiclassical and quantum radiation in the graphene under action of t-step field

© V.V. Dmitriev, D.V. Churochkin, V.A. Tseryupa, S.A. Smolyansky

Saratov National Research State University,
410012 Saratov, Russia
e-mail: dmitrievvv@sgu.ru

Received 2025
Revised 2025
Accepted 2025

We present a kinetic description of quasiclassical and quantum radiation processes in graphene induced by an external field with a specific configuration. As the external perturbation, we employ a constant field of finite duration (so called *t-step pulses*). This choice is motivated by two key considerations: 1) such fields have been previously investigated in related studies, and 2) they can generate transparency windows where the induced radiation exceeds the background field, enabling experimental detection.

Keywords: graphene, kinetic equation.

DOI: 10.61011/TP.2026.05.63512.322-25

Introduction

Graphene has been the focus of active research for decades due to its exceptional properties [1,2]. Its hexagonal crystal structure and symmetry lead to a unique low-energy spectrum in which electrons near Dirac points behave like massless fermions, obeying the linear law of dispersion.

$$\varepsilon(\mathbf{p}) = v_F\sqrt{(p^{(1)})^2 + (p^{(2)})^2}, \tag{1}$$

where $v_F = 10^6$ m/s — Fermi velocity, and $\mathbf{p} = \left(p^{(1)}, p^{(2)}\right)$ — components of a 2D momentum.

This property allows experimental verification of the model at energies significantly lower than those required in quantum electrodynamics. When an external electric field is applied, several amazing quantum vacuum effects occur. For example, Landau-Zener tunneling manifests itself in nonlinear volt-ampere characteristics, providing an insight on the mechanism of electronic transport. In addition, it is possible to study the electromagnetic response or detect radiation emitted by single-layer graphene under the influence of an external laser field.

The current studies of the nonlinear dynamics of graphene include active development of both experimental and theoretical approaches. The possibility of generating high harmonics and nonlinear response in graphene under the action of strong laser pulses in the terahertz range has been demonstrated in [3–5]. In parallel, improved theoretical models are being developed that take into account the relaxation processes [6] and the interelectronic interaction [7] in conditions of strong fields. Of particular interest are recent studies of quantum transport phenomena [8].

In the following analysis, we use a nonperturbative kinetic formalism to study plasma currents in graphene and the corresponding quasiclassical radiation. In addition, we study the case of quantum radiation generated when the charges interact with an external field, focusing exclusively on the annihilation channel in the collision integral.

1. Kinetic equation in graphene

For simplicity, let us consider graphene located in an external linearly polarized homogeneous field with a one-component vector potential $A^\mu = (0, 0, A^{(2)}(t) = A(t), 0)$ in the Hamiltonian calibration $A^{(0)} = 0$. Then the basic kinetic equation of non-Markov type can be written in the integro-differential form [9–12]:

$$\dot{f}(\mathbf{p}, t) = \frac{1}{2}\lambda(\mathbf{p}, t)\int_{t_0}^{t}\lambda(\mathbf{p}, t')[1 - 2f(\mathbf{p}, t')]\cos\theta(\mathbf{p}; t, t')dt' \tag{2}$$

or as an equivalent system of ordinary differential equations

$$\dot{f}(\mathbf{p}, t) = \frac{1}{2}\lambda(\mathbf{p}, t)u(\mathbf{p}, t),$$

$$\dot{u}(\mathbf{p}, t) = \lambda(\mathbf{p}, t)\,[1 - 2f(\mathbf{p}, t)] - \frac{2\varepsilon(\mathbf{p}, t)}{\hbar}\,v(\mathbf{p}, t),$$

$$\dot{v}(\mathbf{p}, t) = \frac{2\varepsilon(\mathbf{p}, t)}{\hbar}\,u(\mathbf{p}, t). \tag{3}$$

Here, we introduce the carrier distribution function $f(\mathbf{p}, t)$ which obeys the elecrto-neutrality condition $f(\mathbf{p}, t) = f_e(\mathbf{p}, t) = f_h(-\mathbf{p}, t)$. Additionally, for the graphene case, we determine the transition amplitude

$$\lambda(\mathbf{p}, t) = \frac{ev_F^2E(t)p_\perp}{\varepsilon^2(\mathbf{p}, t)} \tag{4}$$

and phase

$$\theta(\mathbf{p}; t, t') = \frac{2}{\hbar}\int_{t'}^{t}dt''\varepsilon(\mathbf{p}, t''), \tag{5}$$

where $E(t) = -\frac{1}{c}\dot{A}(t)$ — field strength,
$\varepsilon(\mathbf{p}, t) = v_F\sqrt{p_\perp^2 + P_\parallel^2(t)}$ — quasi-energy,
$P_\parallel(t) = p^{(2)} - \frac{e}{c}A(t)$ — quasi-pulse along the field direction, $p_\perp = p^{(1)}$ — perpendicular component, $e < 0$ — electron charge. Also auxiliary functions that characterize the polarization effects in the system are introduced here.

$$u(\mathbf{p}, t) = \int_{t_0}^{t} \lambda(\mathbf{p}, t')[1 - 2f(\mathbf{p}, t')]\cos\theta(\mathbf{p}; t, t')dt', \quad (6)$$

$$v(\mathbf{p}, t) = \int_{t_0}^{t} \lambda(\mathbf{p}, t')[1 - 2f(\mathbf{p}, t')]\sin\theta(\mathbf{p}; t, t')dt'. \quad (7)$$

Under the initial condition $f(\mathbf{p}, t_0) = u(\mathbf{p}, t_0) = v(\mathbf{p}, t_0) = 0$, we define the integral of motion

$$(1 - 2f)^2 + u^2 + v^2 = 1. \quad (8)$$

The functions discussed above and obtained by analytical or numerical solution of the system are not directly observable experimental quantities. To find a connection with the observed quantities, it is required to consider macroscopic observables such as particle density, currents, and energy characteristics of radiation. As a first step, we define the density of the number of pairs of quasiparticles as

$$n(t) = \frac{N_f}{(2\pi\hbar)^2}\int f(\mathbf{p}, t)d\mathbf{p}, \quad (9)$$

where $N_f = 4$ corresponds to the number of types („aromas“) of quasi-particles in graphene.

Following the conventional definitions, let's introduce the density of current [13]:

$$j_k(t) = -\frac{\delta H(t)}{\delta A_k(t)}. \quad (10)$$

Derivation of the low energy Hamiltonian

$$H(t) = v_F\int \psi^\dagger(\mathbf{x}, t)\hat{\mathbf{P}}\sigma\psi(\mathbf{x}, t)d\mathbf{x} \quad (11)$$

gives the following expression:

$$j_k(t) = N_f e v_F\int \psi^\dagger(\mathbf{x}, t)\sigma_k\psi(\mathbf{x}, t)d\mathbf{x} \quad (12)$$

where σ_k — Pauli matrices ($k = 1, 2$). This current can be expressed as the sum of the conduction current

$$j_\perp^{cond}(t) = \frac{N_f e v_F^2}{(2\pi\hbar)^2}\int \frac{2f(\mathbf{p}, t)p_\perp}{\varepsilon(\mathbf{p}, t)}d\mathbf{p},$$

$$j_\parallel^{cond}(t) = \frac{N_f e v_F^2}{(2\pi\hbar)^2}\int \frac{2f(\mathbf{p}, t)P_\parallel(t)}{\varepsilon(\mathbf{p}, t)}d\mathbf{p}, \quad (13)$$

and polarization current

$$j_\perp^{pol}(t) = -\frac{N_f e v_F^2}{(2\pi\hbar)^2}\int \frac{u(\mathbf{p}, t)P_\parallel(t)}{\varepsilon(\mathbf{p}, t)}d\mathbf{p},$$

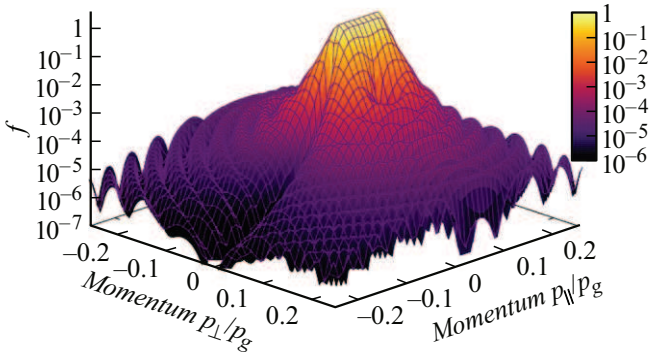

Figure 1. Distribution function under the action of t-step momentum of moderate amplitude and duration ($E_0 = 10^{-3}E_g = 109$kV/cm, $T = 100t_g = 24.6\cdot 10^{-15}$s, $\Longrightarrow \eta = 10$) in the out-state ($t = +T/2$), neglecting the back reaction, $p_g = \hbar/a$ — graphene momentum, $a = 2.46$ A — graphene lattice constant.

$$j_\parallel^{pol}(t) = \frac{N_f e v_F^2}{(2\pi\hbar)^2}\int \frac{u(\mathbf{p}, t)p_\perp}{\varepsilon(\mathbf{p}, t)}d\mathbf{p}. \quad (14)$$

In the context of condensed matter physics, these contributions are traditionally referred to as intra-band and inter-band currents, respectively. The expression related to conduction corresponds to charge transfer by carriers inside individual Dirac cones (conduction band or valence band), whereas the polarization one represents quantum interference between these states, manifested as a trembling motion (Zitterbewegung). In fact, the correct form of the conduction current includes a $(1 - 2f(\mathbf{p}, t))$ multiplier in the numerator, but the constant term vanishes when integrated over the Brillouin zone, taking into account the complete hexagonal lattice of graphene [14].

Note that there are no components of currents (13) and (14) perpendicular to the external electric field: $j_\perp^{cond} = j_\perp^{pol} = 0$. This is due to the fact that the integral functions in $j_\perp^{cond}$ and $j_\perp^{pol}$ are odd functions of the transverse momentum $p_\perp$, and we take the integral over $p_\perp$ within symmetrical limits. The oddness of integral functions — in particular, the oddness of $u(p_\perp)$ and $p_\perp f(p_\perp)$, — can be proved on the basis of kinetic equations (3) taking into account the parity of the quasi-energy ε (1) and the odd amplitude of the transitions λ (4) as functions of the transverse momentum $p_\perp$.

An external t-step momentum generates a certain number of quasiparticles with an asymmetric distribution in the momentum space (Fig. 1). The motion of these charged quasiparticles provides a complex pattern of surface currents. These surface plasma currents, in turn, serve as sources of quasiclassical radiation, which propagates outward on both sides of the graphene plane.

2. Plasma current and quantum transport

Considering graphene as an infinitely thin layer and following the approach [15], we simulate the electromagnetic

field generated by its surface currents. Then, for a surface current that depends on time and current, e.g., flowing along the axis y, $\mathbf{j}(t) = j(t)\mathbf{e}_y$, we get the following expression for the vector potential at a distance of z from the plane:

$$\mathbf{A}_{QCR}(z,t) = \mathbf{e}_y A_{QCR}(z,t) = \mathbf{e}_y \frac{2\pi}{c} \int_z^\infty j\left(t - \frac{\rho}{c}\right) d\rho, \tag{15}$$

where $\rho = \sqrt{x^2 + y^2 + z^2}$. The electric and magnetic field strengths of quasiclassical radiation are equal

$$\mathbf{E}_{QCR}(\tau) = -\mathbf{e}_y \frac{1}{c} \frac{\partial A_{QCR}}{\partial t} = -\mathbf{e}_y \frac{2\pi}{c} j(\tau),$$

$$\mathbf{B}_{QCR}(z,t) = -\mathbf{e}_x \frac{\partial A_{QCR}}{\partial z} = \mathbf{e}_x \frac{2\pi}{c} j(\tau)\,\mathrm{sign}(z), \tag{16}$$

where $\tau = t - \rho/c$ — delayed time. Poynting vector of radiation is equal

$$\begin{aligned} \mathbf{S}_{QCR}(z,t) &= \frac{c}{4\pi} \mathbf{E}_{QCR}(\tau) \times \mathbf{B}_{QCR}(z,t) \\ &= \mathbf{e}_z \frac{c}{4\pi} E_{QCR}(\tau) B_{QCR}(z,t), \end{aligned} \tag{17}$$

so the energy of quasiclassical radiation per unit time passing through a unit area at a height of z above the graphene layer is equal to

$$|\mathbf{S}_{QCR}(z,t)| = \frac{\pi}{c} j^2(\tau). \tag{18}$$

As can be seen from Fig. 2, the quasiclassical electric field remains nonzero even after the external field is turned off ($t \gg T$), which leads to an unlimited increase in

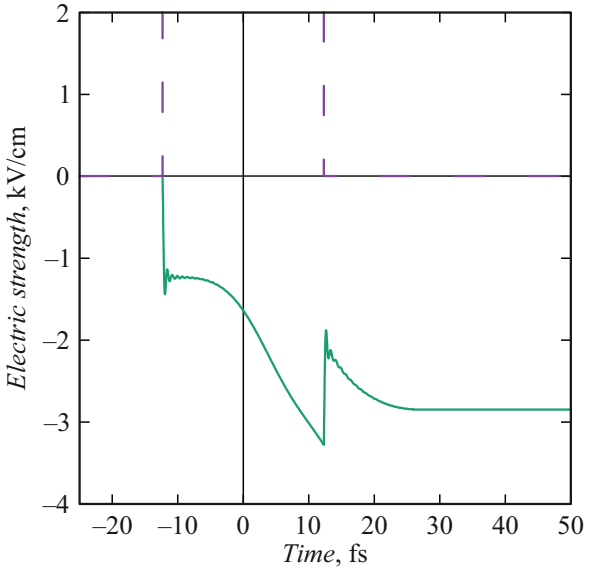

Figure 2. Evolution of electric field strength under the action of t-step momentum with an amplitude of $E_0 = 10^{-3}E_g = 109$kV/cm and a duration of $T = 100t_g = 24.6 \cdot 10^{-15}$s, neglecting the back reaction. Solid line — quasiclassical radiation E_{QCR} in the graphene plane ($z = 0$); dashed line — external field (t-step momentum).

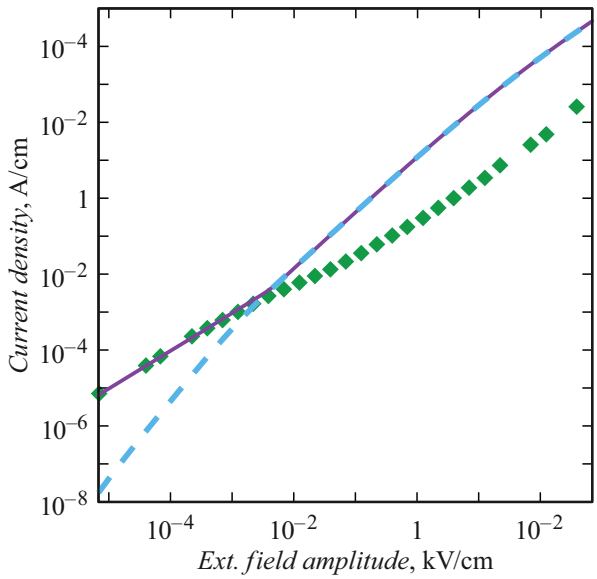

Figure 3. „Current-voltage relation“ — the amplitude of the current density as a function of the amplitude of t-step pulse at $T = 4 \cdot 10^3 t_g = 10^{-12}$s, taking into account the feedback. Dashed line — conductivity current $\max\limits_t |j_{cond}(t)|$; dotted line — polarization current $\max\limits_t |j_{pol}(t)|$; solid line — full current $\max\limits_t |j_{cond}(t) + j_{pol}(t)|$.

radiated energy ($\int |\mathbf{S}| dt$) and thereby reveals a fundamental limitation of the model. To eliminate this shortcoming, it is necessary to include the effects of a back reaction.

Nevertheless, even this numerical model provides a valuable insight into the relationship between surface currents and the parameters of the external field. Consequently, it gives a preliminary understanding of quantum transport in graphene structures, while requiring knowledge of only the most fundamental property of its low-energy model, the linear law of dispersion. Accroding to [16], we introduce the dimensionless parameter η, describing the field „intensity“ and determining the charge transfer condition.

$$\frac{\eta}{2\pi} = \frac{E_0}{E_g} \left(\frac{T}{t_g}\right)^2, \tag{19}$$

where graphene units are introduced: intensity $E_g = \hbar v_F/(|e|a^2) = 1.089 \cdot 10^8$V/cm, time $t_g = a/v_F = 2.46 \cdot 10^{-16}$s, and $a = 2.46$A denotes graphene lattice constant.

The calculated results in Fig. 3 show two specific transport modes. Within the weak field $\eta \ll 1$, the system is described by the linear Kubo [2] response theory and demonstrates compliance with Ohm law, with the polarization current dominating. In contrast to this mode, the mode of strong field $\eta \gg 1$ has a non-linear dependence $E^{3/2}$. It comes from the intense generation of quasi-particles through the Schwinger mechanism, which leads to the dominance of the conduction current over the polarization current and provides a nonlinear transport mechanism. The

temporal dynamics of the system is controlled by Landau-Zener transitions, in which the processes of interband tunneling are suppressed in favor of intraband conduction as the electric field strength goes up. In previous studies that studied similar effects of fields in graphene [14,16,17] and the Kibble-Zurek mechanism [18,19], a similar type of dependence $\sim tE^{3/2}$ was obtained.

3. Quasiclassical radiation

For further analysis, we adopt two key simplifying approximations [20]. First, we use the low-density approximation, which corresponds to the condition $f(\mathbf{p}, t) \ll 1$ on the right side of kinetic equation (2). This corresponds to the case of a low quasi-particles production rate. Eventually, we get the distribution function as

$$f^{(LD)}(\mathbf{p}, t) = \frac{1}{4}\left|\hat{\lambda}(\mathbf{p}, t)\right|^2, \tag{20}$$

where

$$\hat{\lambda}(\mathbf{p}, t) = \int_{t_0}^{t} dt' \lambda(\mathbf{p}, t') \exp\left[-i\frac{2}{\hbar}\int_{t'}^{t} dt'' \varepsilon(\mathbf{p}, t'')\right]. \tag{21}$$

Formulas (20) and (21) are valid for the quasi-energy $\varepsilon(\mathbf{p}, t)$ and the amplitude of transitions $\lambda(\mathbf{p}, t)$ of any kind (e.g., linear or nonlinear in momentum). $f^{(LD)} \ll 1$ condition must be fulfilled.

The second simplification is a weak field approximation:

$$\left|\frac{e}{c}\mathbf{A}(t)\right| \ll |\mathbf{p}|, \quad \forall t. \tag{22}$$

It simplifies the quasi-energy and transitions amplitude:

$$\varepsilon(\mathbf{p}, t) \to \varepsilon^{(0)}(p) = v_F|\mathbf{p}|, \tag{23}$$

$$\lambda(\mathbf{p}, t) \to \lambda^{(0)}(\mathbf{p}, t) = \frac{e v_F^2 p_\perp}{[\varepsilon^{(0)}(p)]^2}\,\mathrm{E}(t) = \frac{e\sin\varphi}{p}\,\mathrm{E}(t), \tag{24}$$

where φ — angle between $\mathbf{p}$ and $\mathbf{E}$ (both vectors — in graphene plane).

By combining two approximations we get

$$f^{(LD,0)}(\mathbf{p}, t) = \left|\frac{e v_F^2 p_\perp}{2\varepsilon^{(0)}(p)}\tilde{E}(\nu, t)\right|^2_{\nu=\varepsilon^{(0)}/\pi\hbar}, \tag{25}$$

where

$$\tilde{E}(\nu, t) = \int_{t_0}^{t} dt' E(t') \exp(-2\pi i \nu t') \tag{26}$$

is a window Fourier transform (WFT) or a short-term Fourier transform (STFT).

The energy density of the electron-hole plasma is equal

$$\mathcal{E}^{(LD,0)}(t) = \frac{2N_f}{(2\pi\hbar)^2}\int \varepsilon^{(0)}(p) f^{(LD,0)}(\mathbf{p}, t) d\mathbf{p}. \tag{27}$$

By substituting the distribution function (24) here, let's go to the polar coordinate system $(|\mathbf{p}|, \varphi)$, and integrate by azimuth φ. As a result

$$\mathcal{E}^{(LD,0)}(t) = \frac{e^2}{2\hbar}\int_0^\infty d\nu \left|\tilde{E}(\nu, t)\right|^2. \tag{28}$$

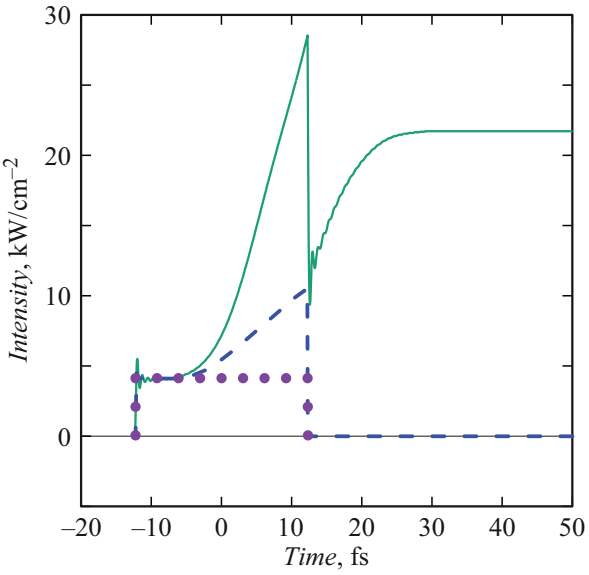

Figure 4. Evolution of intensities under the action of t-step momentum (with parameters as shown in Fig. 1, 2) without taking into account the back reaction. Solid line — intensity of quasiclassical radiation $|\mathbf{S}_{QCR}|$; dashed line — surface density of the quasi-particles' power $\dot{\mathcal{E}}_{eh}$, multiplied (for comparison) by $\pi\alpha/4 \approx 5.7 \cdot 10^{-3}$; dotted line — external field intensity $|\mathbf{S}_{ext}|$, multiplied by $(\pi\alpha/2)^2 \approx 1.3 \cdot 10^{-4}$. Almost everywhere in the graph (except for $t \geq T/2 = 12.3 \cdot 10^{-15}$s, where external field is deactivated) the following is fulfilled: $|\mathbf{S}_{QCR}| \ll \dot{\mathcal{E}}_{eh} \ll |\mathbf{S}_{ext}|$.

Using the energy flow of an electromagnetic wave, it is possible to rewrite the energy density using Poynting vector (17) as

$$\mathcal{E}^{(LD,0)}(t) = \frac{\pi e^2}{\hbar c}\int_{-\infty}^{t} |\mathbf{S}(t')|\, dt'. \tag{29}$$

This analytical evaluation shows that only $\pi/137 \sim 2.2\,\%$ of incident electromagnetic energy is absorbed by graphene. This is in excellent agreement with the experimental data on optical transparency of the graphene monolayer [21]. Data of computational modeling of quasiclassical radiation under the action of a t-step momentum are shown in Fig. 4.

4. Quantum radiation

The interaction of the electron-hole plasma (EHP) with the photon field generates quantum radiation. The corresponding kinetic equations for the EHP and the photonic subsystem in graphene were obtained in work [11] using a dynamic approach similar to the kinetic theory of electron-positron-photon plasmas in strong external fields [22]. We will consider below only the annihilation channel in the integral of photon collisions, neglecting the back reaction of the electron-hole pairs created as a result of photon absorption.

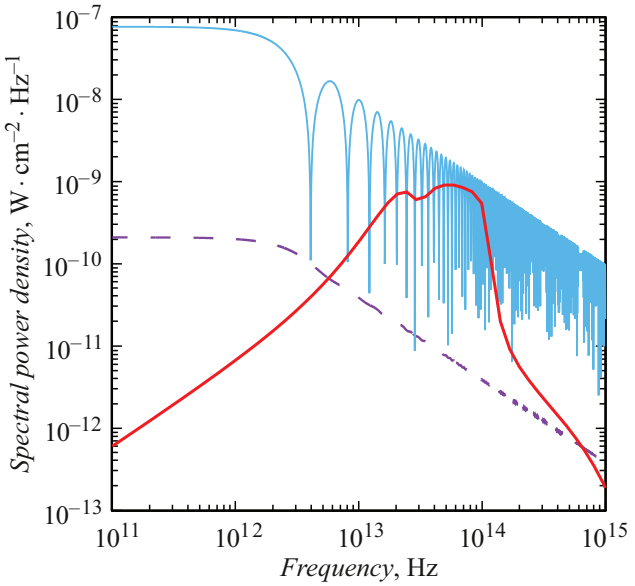

Figure 5. Spectral power density under the action of strong T —-const field ($E_0 = 10^{-4}E_g \approx 10$kV/cm, $T = 10^3 t_g = 2.46 \cdot 10^{-13}$s) in the moment $t = T$ providing for back-reaction ($\mathbf{E} = \mathbf{E}_{ext} + \mathbf{E}_{int}$). Solid oscillating line — external field (T-const); dashed line — quasiclassical radiation $\left|\tilde{\mathbf{S}}_{QCR}(\nu)\right|$ at $z = 0$; solid smooth line — quantum radiation (QR) $\dot{\mathcal{E}}_{ph,\nu}(\nu) \cdot d$. QR is calculated from the system of equations (30) in the low photon density approximation ($F \ll 1$).

The corresponding system of ordinary differential equations takes the following form:

$$\dot{F}(\mathbf{K}, t) = \Lambda(K) \int \frac{d^2p}{(2\pi\hbar)^2} U(\mathbf{p}, \mathbf{K}, t),$$

$$\dot{U}(\mathbf{p}, \mathbf{K}, t) = [f(\mathbf{p}, t) + f(\mathbf{p} + \mathbf{K}, t) - 1] F(\mathbf{K}, t) + f(\mathbf{p}, t) f(\mathbf{p} + \mathbf{K}, t) - \frac{1}{\hbar} [\varepsilon(\mathbf{p}, \tau) + \varepsilon(\mathbf{p} + \mathbf{K}, t) - cK] V(\mathbf{p}, \mathbf{K}, t),$$

$$\dot{V}(\mathbf{p}, \mathbf{K}, t) = \frac{1}{\hbar} [\varepsilon(\mathbf{p}, t) + \varepsilon(\mathbf{p} + \mathbf{K}, t) - cK] U(\mathbf{p}, \mathbf{K}, t), \quad (30)$$

where $\mathbf{K} = (\mathbf{k}, k^{(3)})$ denotes a 3D photon momentum (where $\mathbf{k}$ gives components in plane, and $k^{(3)}$ — component normal to the graphene plane), $K = |\mathbf{K}|$, and amplitude

$$\Lambda(K) = \frac{(ev_F)^2}{cKd}, \quad (31)$$

where $d = a = 2.46$ A — thickness of graphene layer.

According to the photons distribution function $F(\mathbf{K}, t)$, the volumetric density of all photons $n_{ph}(t)$ is the integral of function $F(\mathbf{K}, t)$ over the space of photon momentum $\mathbf{K}$ ($\mathbf{K} \in \mathrm{R}^3$):

$$n_{ph}(t) = \int d^3K \; n_{ph,\mathbf{K}}(\mathbf{K}, t), \quad (32)$$

where

$$n_{ph,\mathbf{K}}(\mathbf{K}, t) = \frac{N_f}{(2\pi\hbar)^3} F(\mathbf{K}, t) \quad (33)$$

— spectral (photon momentum vector differential) volume density of the number of photons,

$$[n_{ph,\mathbf{K}}] = [\text{length}^{-3} \cdot \text{momentum}^{-3}].$$

The volumetric energy density of all photons [energy · length^{-3}] is, by definition,

$$\mathcal{E}_{ph}(t) = \int d^3K \; \mathcal{E}_{ph,\mathbf{K}}(\mathbf{K}, t), \quad (34)$$

where

$$\mathcal{E}_{ph,\mathbf{K}}(\mathbf{K}, t) = cKn_{ph,\mathbf{K}}(\mathbf{K}, t) = \frac{N_f cK}{(2\pi\hbar)^3} F(\mathbf{K}, t) \quad (35)$$

— spectral (photon momentum vector differential) volumetric photon energy density,

$$[\mathcal{E}_{ph,\mathbf{K}}] = [\text{energy} \cdot \text{length}^{-3} \cdot \text{momentum}^{-3}].$$

In order to compare the spectra of quasiclassical and quantum radiation, it is convenient to introduce the volumetric energy density of photons, differential in their frequency ν ($\nu = cK/h$), $\mathcal{E}_{ph,\nu}(\nu, t)$, subjecting it to the condition:

$$\int_0^\infty d\nu \; \mathcal{E}_{ph,\nu}(\nu, t) = \mathcal{E}_{ph}(t). \quad (36)$$

Comparing this definition (identity) with the energy density of all photons $\mathcal{E}_{ph}$ (34), we find a relationship between the differential energy density of photons $\mathcal{E}_{ph,\nu}$ and their distribution function F:

$$\mathcal{E}_{ph,\nu}(\nu, t) = \frac{2\pi\hbar}{c} K^2 \int d\Omega \, \mathcal{E}_{ph,\mathbf{K}}(\mathbf{K}, t)\Big|_{K=2\pi\hbar\nu/c} = N_f \frac{K^3}{(2\pi\hbar)^2} \int d\Omega \, F(\mathbf{K}, t)\Big|_{K=2\pi\hbar\nu/c}, \quad (37)$$

where integral is taken over solid angle Ω of the entire sphere.

The value $\dot{\mathcal{E}}_{ph,\nu}(\nu, t)$ we call the power spectrum of quantum radiation. It has the following size power · length^{-3} · frequency^{-1}.

We call the intensity spectrum of quasiclassical radiation the absolute value of the window Fourier transform over the absolute value of the Poynting vector (17):

$$\left|\tilde{\mathbf{S}}_{QCR}(\nu, t)\right| = \left|\int_{-\infty}^{t} dt' |\mathbf{S}_{QCR}(t')| \exp(-2\pi i \nu t')\right|. \quad (38)$$

It has the following dimension power·length^{-2}·frequency^{-1}.

To compare the spectra of quantum and quasiclassical radiation and to adjust their dimensions, we multiply the spectrum of quantum radiation $\dot{\mathcal{E}}_{ph,\nu}(\nu, t)$ by the thickness of the graphene layer d.

In Fig. 5, we expect to see „transparency windows“ for t-step momentum, which can be observed experimentally, i.e. frequency ranges in which the induced radiation exceeds the intensity of the external field.

Conclusion

In this paper, a consistent kinetic theory has been developed that describes the processes of radiation in graphene under the action of stepwise momentum. The main scientific result is the creation of a self-consistent model combining a nonperturbative description of the generation of electron-hole pairs, the generation of quasiclassical radiation by plasma currents and quantum radiation in the annihilation channel. Within the proposed method, the quantitative patterns of transition between the modes of dominance of the polarization current and the conduction current have been established.

The achieved level of dynamic representation of radiation in graphene not only demonstrates qualitative consistency with experimental results but also forms a methodological basis for describing nonstationary phenomena in graphene and opens up prospects for further research of nonlinear radiation processes in strong fields of complex time configuration.

Conflict of interest

The authors declare that they have no conflict of interest.

References

[1] K.S. Novoselov, A.K. Geim, S.V. Morozov, D. Jiang, M.I. Katsnelson, I.V. Grigorieva, S.V. Dubonos, A.A. Firsov. Nature, **438** (7065), 197 (2005).
[2] A.H. Castro Neto, F. Guinea, N.M.R. Peres, K.S. Novoselov, A.K. Geim. Rev. Mod. Phys., **81** (1), 109 (2009).
[3] S. Rakhmanov, K. Matchonov, H. Yusupov, K. Nasriddinov, D. Matrasulov. Eur. Phys. J. B, **98** (2), 35 (2025).
[4] G. Soavi, G. Wang, H. Rostami, D.G. Purdie, D.De Fazio, T. Ma, B. Luo, J. Wang, A.K. Ott, D. Yoon, S.A. Bourelle, J.E. Muench, I. Goykhman, S.D. Conte, M. Celebrano, A. Tomadin, M. Polini, G. Cerullo, A.C. Ferrari. Nature Nanotechnol., **13** (7), 583 (2018).
[5] H.A. Hafez, S. Kovalev, J.C. Deinert, Z. Mics, B. Green, N. Awari, M. Chen, S. Germanskiy, U. Lehnert, J. Teichert, Z. Wang, K.J. Tielrooij, Z. Liu, Z. Chen, A. Narita, K. Müllen, M. Bonn, M. Gensch, D. Turchinovich. Nature, **561** (7724), 507 (2018).
[6] J.A. Canas, D.A. Bonilla, A. Martín-Ruiz. Phys. Rev. B, **112** (10) 104206 (2025).
[7] P. Kumar, T.M. Herath, V. Apalko. J. Phys.: Condens. Matter., **33** (33), 335305 (2021).
[8] G Trambly de Laissardière, et al. Physica E-Low-Dimensional Systems and Nanostructures, 175, 116362 (2026).
[9] S.A. Smolyansky, A. Panferov, D. Blaschke, N. Gevorgayn. Particles, **2** (2), 208 (2019).
[10] S.A. Smolyansky, A.D. Panferov, D.B. Blaschke, N.T. Gevorgyan. Particles, **3** (2), 456 (2020).
[11] S.P. Gavrilov, D.M. Gitman, V.V. Dmitriev, A.D. Panferov, S.A. Smolyansky. Universe, **6** (11), 205 (2020).
[12] A.D. Panferov, D.V. Churochkin, A.M. Fedotov, S.A. Smolyansky, D.B. Blaschke, N.T. Gevorgyan. In *Proceedings of the Ginzburg Centennial Conference on Physics*, (May 29–June 3, 2017, Moscow). http://gc2.lpi.ru/proceedings/panferov.pdf Last accessed 16 March 2020
[13] P. Martin, J. Schwinger. Phys. Rev., **115** (6), 1342 (1959).
[14] B. Dora, R. Moessner. Phys. Rev. B, **81** (16), 165431 (2010).
[15] T.A. Abbott, D.J. Griffiths. Am. J. Phys., **53** (12), 1203 (1985).
[16] G.L. Klimchitskaya, V.M. Mostepanenko. Phys. Rev. D, **87** (12), 125011 (2013).
[17] S.P. Gavrilov, D.M. Gitman, N. Yokomizo. Phys. Rev. D, **86** (12), 125022 (2012).
[18] T.W.B. Kibble. J. Phys. A, **9** (8), 1387 (1976).
[19] W.H. Zurek. Nature, **317** (6037), 505 (1985).
[20] D.B. Blaschke, V.V. Dmitriev, N.T. Gevorgyan, B. Mahato, A.D. Panferov. Springer Proc. Phys., **281** 187 (2022).
[21] R.R. Nair, P. Blake, A.N. Grigorenko, K.S. Novoselov, T.J. Booth, T. Stauber, N.M.R. Peres, A.K. Geim. Science, **320** (5881), 1308 (2008).
[22] D.B. Blaschke, V.V. Dmitriev, G. Roepke, S.A. Smolyansky. Phys. Rev. D, **84** (8), 085028 (2011).
[23] I.V. Oladyshkin, S.B. Bodrov, A.V. Korzhimanov, A.A. Murzanev, Yu.A. Sergeev, A.I. Korytin, M.D. Tokman, A.N. Stepanov. Phys. Rev. B, **106** (20), 205407 (2022).

Translated by T.Zorina